RESEARCH ARTICLE   OPEN ACCESS

Measuring the Thermal Conductivities of Low Heat Conducting Disk Samples by Monitoring the Heat Flow

[1]José A. Ibáñez-Mengual* [1]Ramón Valerdi-Pérez y [1]José A. García-Gamuz

[1]*Departamento de Física, Universidad de Murcia, Campus de Espinardo, 30071 Murcia*

ABSTRACT
This article aims to establish an experimental procedure to measure heat transmission coefficients in low heat conductive materials. The newly developed model takes as starting point the application of Fourier's law to a disk sample when a temperature gradient is established between its faces. The power of a heating element is determined as the heat transfer coefficient of the problem disk. Initially, a glass vessel containing water is placed in direct contact with the heating element; then, a problem plastic disk is placed between this element and the glass vessel, treating the set as a composite wall. Prior to the above the water equivalent of a calorimetric set (vessel + water + accessories) and the thermal conductivity of the vessel must be determined. The thermal conductivity of the problem plastic disk sample is obtained for temperatures ranging from 30 to 70° C. The results reveal the existence of some type of structural transition for the problem material.
*Keywords***:** thermal conductivity; heat flow; plastic material.

I.   INTRODUCTION

The problem of heat conduction in solids has been widely studied, and many solutions are available for various boundary conditions, forms and dimensions. Measurement of the thermal properties of a material is an important issue since the parameters associated with it are extremely relevant both in the laboratory and in industrial design [1] [2].

The direct measurement of heat transfer has been studied using several techniques, including the use of circular heat flow discs, thermistors, as well as comparisons and calibrations of heat flux sensors [3] [4]. The devices and techniques studied include differential scanning calorimeters, improved thin film heat transfer gauges, infrared thermography [5] and liquid crystals [6] and several other visualization techniques [7]. The techniques involved are used for direct measurement of the temperature with thin film thermocouples [8], sputtered micro thermocouples, thermo fluorescence [9], thin-foil thermography [10] and fine wire thermocouples for transient measurement.

Thermal conductivity [11] [12] has been studied for a wide variety of materials [13] [14] [15] [16] using various experimental techniques, such as transient plane source, pulsed and thermal quadruples, electrical resistance thermometry [17], transient and parallel hot wire techniques, infrared thermography, laser flash, photoacoustics, etc.

The study in this case is directed towards plastic materials. Due to the great variety of new products intended for recycling, the rapid and accurate determination of their thermal properties is of great importance [18] [19] [20] [21] [22]. The aim of the experiments described was to design a modified Lee's disk method for measuring thermal conductivities in samples of low heat conducting materials. [23] [24] [25] [26].

II.   THEORY

In the case of water (mass *m*) in a glass vessel placed on a heating element at temperature θ_c > θ_a (room temperature), as in Figure 1, the power transferred corresponds to the heat gained due to losses from the system, characterized by λ_1 and λ_2 coefficients respectively, resulting in the following equation,

$$\frac{\delta Q}{dt}=\left(mc_a+k\right)\frac{d\theta}{dt}=C\frac{d\theta}{dt}=\left(\frac{\delta Q}{dt}\right)_1+\left(\frac{\delta Q}{dt}\right)_2=-\lambda_1\left(\theta-\theta_c\right)-\lambda_2\left(\theta-\theta_a\right)$$

(1)

where $(\delta Q/dt)_1$ and $(\delta Q/dt)_2$ are the net power entering the system from the heating element and the losses respectively, θ is its temperature, $C \equiv mc_a + k$ is the heat capacity of the system (c_a the specific heat of water) and k the water equivalent of the same, which corresponds to the heat capacity of the surrounding vessel, as well as of the measuring probe (accessories). Regrouping terms in the above equation gives

$$-\left(\lambda_1+\lambda_2\right)\theta+\lambda_1\theta_c+\lambda_2\theta_a=C\frac{d\theta}{dt},$$

Introducing $\alpha \equiv \lambda_1 + \lambda_2$, and $\gamma \equiv \lambda_1\theta_c + \lambda_2\theta_a$, it follows that

$$C\frac{d\theta}{dt}=-\alpha\theta+\gamma \quad \Rightarrow \quad \frac{d\theta}{\gamma-\alpha\theta}=\frac{dt}{C}=\beta dt$$

(2)

with $\beta = C^{-1}$. Integrating the above equation between the initial temperature (θ_a) and the temperature (θ) reached at the end of a given time *t*, yields
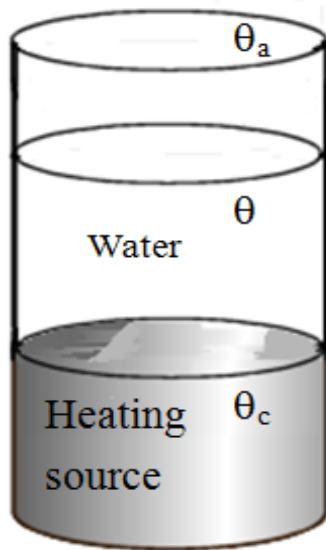
Figure 1. Heating source + water + system

$$\int_{\theta_a}^{\theta} \frac{-\alpha \cdot d\theta}{\gamma - \alpha\theta} = -\alpha\beta t \quad \Rightarrow \quad \ln\left[\frac{\gamma - \alpha\theta}{\gamma - \alpha\theta_a}\right] = -\alpha\beta t \quad \Rightarrow \quad \alpha\theta - \gamma = (\alpha\theta_a - \gamma)\left[\exp(-\alpha\beta t)\right] \quad \Rightarrow$$

$$\Rightarrow \quad \theta = \frac{\gamma}{\alpha} - \left(\frac{\gamma}{\alpha} - \theta_a\right)\left[\exp(-\alpha\beta t)\right]$$

(3)

so that, if the boundary conditions of the system are applied ($t \to 0$, $\theta = \theta_a$ and $t \to \infty$, $\theta = \theta_f = (\gamma/\alpha)$ (final temperature)), eq. (3) can be written as

$$\theta = \theta_f - \left[(\theta_f - \theta_a)\exp(-\alpha\beta t)\right] \quad \Rightarrow \quad \theta = \theta_f - \left[(\theta_f - \theta_a)\exp(-bt)\right]$$

with $b = \alpha \cdot \beta = \dfrac{\alpha}{C} = \dfrac{\lambda_1 + \lambda_2}{C}$

This equation is of the form

$$\theta = c - \left[a \cdot \exp(-bt)\right] \qquad , \qquad \text{being}$$

$$\begin{cases} c = \theta_f = \dfrac{\gamma}{\alpha} = \dfrac{\lambda_1\theta_c + \lambda_2\theta_a}{\lambda_1 + \lambda_2} \\[3mm] a = \theta_f - \theta_a = \dfrac{\lambda_1(\theta_c - \theta_a)}{\lambda_1 + \lambda_2} \end{cases}$$

(4)

from where it immediately follows

$$(\lambda_1 + \lambda_2)\theta_f = \lambda_1\theta_c + \lambda_2\theta_a \quad \Rightarrow \quad \frac{\lambda_2}{\lambda_1} = \frac{\theta_f - \theta_c}{\theta_a - \theta_f}$$

(5)

and $C \cdot b = \lambda_1 + \lambda_2$ (6)

The final reduced temperature

$\overline{\theta}_f \equiv (\theta_f - \theta_c)/(\theta_a - \theta_f)$ and $\overline{C} \equiv C \cdot b$. Taking into account eqs. (6) and (5) yields an equation

system, whose resolution provides expressions for the coefficients λ_1 and λ_2:

$$\left.\begin{array}{l} \lambda_1 = \dfrac{\overline{C}}{1 + \overline{\theta}_f} \\[5mm] \lambda_2 = \lambda_1 \overline{\theta}_f \end{array}\right\}$$

(7)

Equations (7) correspond to the gain and loss coefficients of the system, whose values give the power supplied by the heating element, in accordance with eq. (1). In particular, if we consider that a sufficient time interval has passed to reach the steady state ($\theta = \theta_f$), of the net heat transfer is cancelled, so that ($\delta Q/dt$)= 0 and the power supplied by the heating element is

$$\left(\frac{\delta Q}{dt}\right)_1 = \lambda_1(\theta_c - \theta_f)$$

(8)

2.1. Determination of water equivalent by the mixtures method.

To calculate the power supplied by the heating element, it is necessary to know the water equivalent value of the system k. For this, it is possible to use the mixtures method; witch consists of introducing a known metal body (copper disk) in the glass vessel containing water at room temperature [27]. The body is previously heated to reach the boiling point of water (100ºC at normal atmospheric pressure). In this way it is possible to know the temperature of the material in the water, whose temperature increases. The metal is removed from the water at the end of time interval Δt and consequently the water temperature decreases due to the cooling effect of its surroundings. Figure 2 outlines the thermogram corresponding to the full process, which shows three stages: pre-heating, heating and post-heating which, in our case, lasted 20, 1 and 20 minutes, respectively (Figure 3).
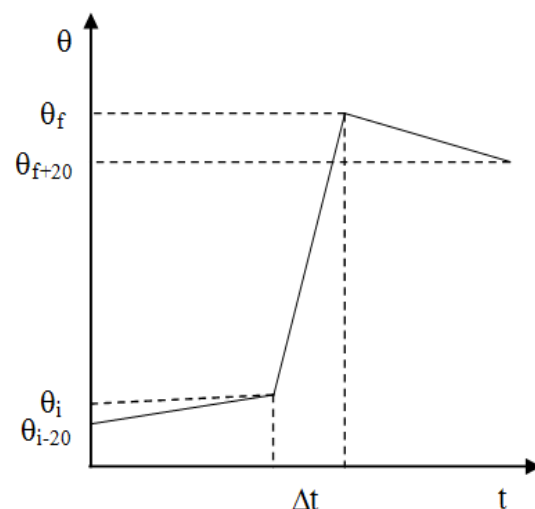

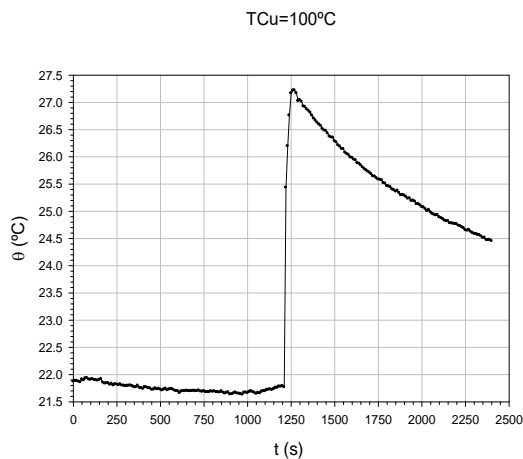**Figure 2.** Full process thermogram.

TCu=100ºC

Figure 3. Thermogram for the water equivalent determination. A copper disk of 43.5 g was used.

The heat balance equation corresponding to the heating stage can be written as

$$Mc_M(\theta_f-\theta_i)=(m_ac_a+k)(\theta_f-\theta_i)+\dot{Q}_p\Delta t$$

(9)

where *M* is the body mass, c_M its specific heats, m_a is the water mass, c_a the water specific heat capacity, θ_i and θ_f are the initial and final temperature corresponding to the heating time interval *Δt*, and $\dot{Q}_p$ indicates the losses of heat per unit of time in this stage, which can be estimated as the arithmetic mean of the exchanges associated to the pre-heating and post-heating stages,

$$\dot{Q}_p=\frac{\dot{Q}_p^{pre}+\dot{Q}_p^{post}}{2}\begin{cases}\dot{Q}_p^{pre}=(m_ac_a+k)\left[\frac{[(\theta_i-\theta_{i-20})]}{20}\right]\\\dot{Q}_p^{post}=(m_ac_a+k)\left[\frac{[(\theta_{f+20}-\theta_f)]}{20}\right]\end{cases}$$

where $\dot{Q}_p^{pre}$ corresponds to thermal stabilization of the glass vessel + water system at temperature θ_a with θ_{i-20} and θ_i are the initial and final temperature of this stage and $\dot{Q}_p^{post}$ is the heat lost when the metal body is removed and the water temperature approaches the surrounding temperature, θ_f and θ_{f+20} are the initial and final temperatures of the stage.

Thus, the energy balance given by equation (9) can be rewritten as

$$Mc_M(\theta_f-\theta_i)=(m_ac_a+k)\left[(\theta_f-\theta_i)+\frac{[(\theta_f-\theta_{i-20})+(\theta_{f+20}-\theta_i)]}{40}\right]$$

(10)

Equation (10) enables us to determine the water equivalent *k* value, since we know mass and specific heat capacity of the metal body employed.

2.2. Thickness and thermal conductivity calculation for problem materials. Composed wall method.

When a problem material disk sample, whose heat transmission coefficient we wish to know, is placed between a heating source and a glass vessel with water, the system corresponds to a composed wall arranged as shown in Figure 4 where k_1 and k_2 are thermal conductivities and δ_1 and δ_2 thicknesses, respectively, θ_i^* (i=1,2,3) represents temperatures at the three interfaces: 1) heating source/sample material; 2) sample material/glass layer; 3) glass layer/water (see Figure 5). The superscript * will be used to indicate that the affected quantities refer to the problem material disk. Given that in the steady state the heat flow is the same through every element of the composed wall, we can write

$$pot^*\equiv\left(\frac{\delta Q}{dt}\right)^*=\frac{\theta_1^*-\theta_2^*}{\frac{\delta_1}{k_1A}}=\frac{\theta_3^*-\theta_2^*}{\frac{\delta_2}{k_2A}}=\frac{\left(\theta_1^*-\theta_2^*\right)A}{\left[\frac{\delta_1}{k_1}+\frac{\delta_2}{k_2}\right]}$$

(11)

where "*pot**" denotes the dissipated power by the heating source towards the system, A being the common area of different interfaces.
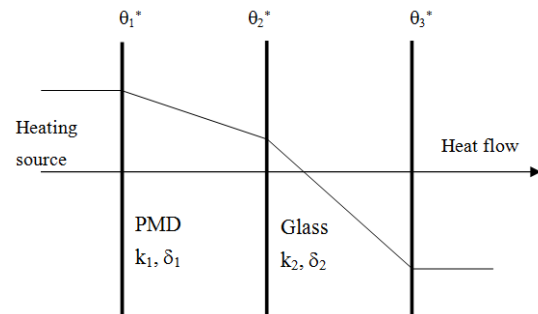

Figure 4. Wall composed of two layers: problem material and glass. Profile of temperature in steady state.
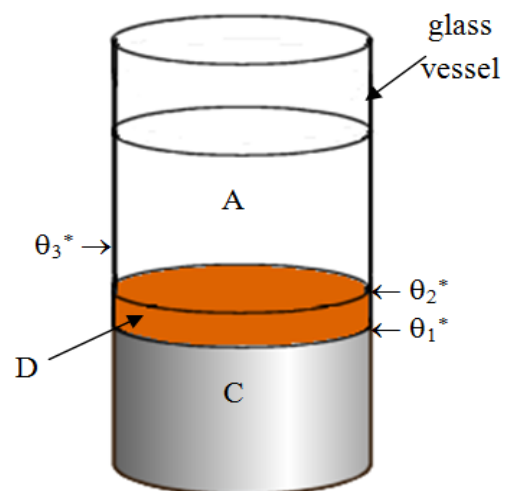

Figure 5. Experimental setup: water in glass vessel (A), disk (D) and cylindrical heating source (C).

When the glass vessel with water is placed in direct contact with the heating source, the power supplied by the source (*pot*) is given by the expression

$$pot \equiv \left(\frac{dQ}{dt}\right) = k_2 \frac{A}{\delta_1}(\theta_2 - \theta_1) \qquad (12)$$

θ_2 being the temperature at the top of the glass vessel (at the interface glass/water).

The thermal conductivity of the glass (k_2) is determined from equation (12), if the thickness δ_2 is known so that it is possible to obtain the thermal conductivity of the problem material (k_1) from equation (11)

$$k_1 = \frac{pot^* \cdot \delta_1 k_2}{\left(\theta_1^* - \theta_2^*\right) A \cdot k_2 - \delta_2 \cdot pot} \qquad (13)$$

III.   EXPERIMENTAL DEVICE

An experimental device was designed, which enables a problem disk of suitable dimension ($\varnothing$ 3 *cm*, thickness 2 *mm*) to be manipulated (see Figure 6). The disk was placed on top of an aluminum cylinder of 2 *cm* thickness. The cylinder is insulated with armaflex, and an electrical resistance placed within is used as heating element. The heating source temperature θ_c is determined by a type J thermocouple (iron-constantan, range -210 to 1200 ºC) lodged in the aluminum cylinder. The resistance and thermocouple are connected to a control device, provided with a screen that shows instantaneous values of the heating cylinder temperature, θ_c, which is the parameter that governs and regulates the heating of the system. Another J thermocouple continuously measures the temperature of the deionized water (40 cm^3), θ, contained in a glass vessel (wall thickness 2 *mm*) placed on of the heating cylinder. This temperature reaches a final value θ_f for every θ_c considered. The surface temperature values of the heating cylinder (θ_r), for every θ_c value selected, was determined by means of an infrared thermometer with configured emissivity (in our case, an Optris® LS thermometer with infrared dual focus), provided with a laser indication device that directs a beam at the top of the problem body (shaping a cross oriented to the center of the disk)). This provided a guide for the optimal measuring distance (object distance (D) and focal measurement area (S), whose D:S ratio in our case is 75:1 for the disk used).
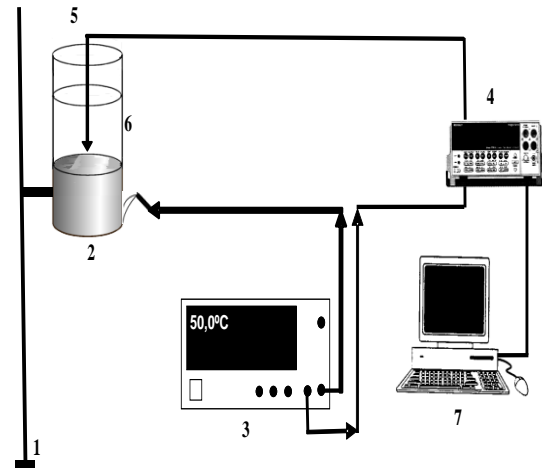

Figure 6. Experimental setup: 1) Support. 2) Heating cylinder with insulating wrapping material. 3) Heat control device. Display with reference temperature. 4) Multimeter. 5) Thermal probe in water. 6) Glass vessel. 7) PC.

IV.   RESULTS AND DISCUSSION

Equation (10) enables the determination of the water equivalent of our calorimetric set *k* (14,623 g) and consequently the heat capacity, *C*, whose value (64,623 cal g^{-1} ºC^{-1}), together with *b* in the exponential fitting (see eq. (4)) for the corresponding water thermogram (glass vessel + water). Figure 7 shows the result obtained for reference temperature θ_c =50ºC. When temperature θ_c ranges between 30 and 70ºC (5ºC steps), the coefficients λ_1 and λ_2 can be determined (see eq. 7). According to eq. (8), in this case (glass) the power ($\delta Q/dt$)= λ_1 (θ_c- θ_f) in eq. (12) gives the glass heat conductivity k_2, knowing the thickness δ_2. These results are listed in Table 1.
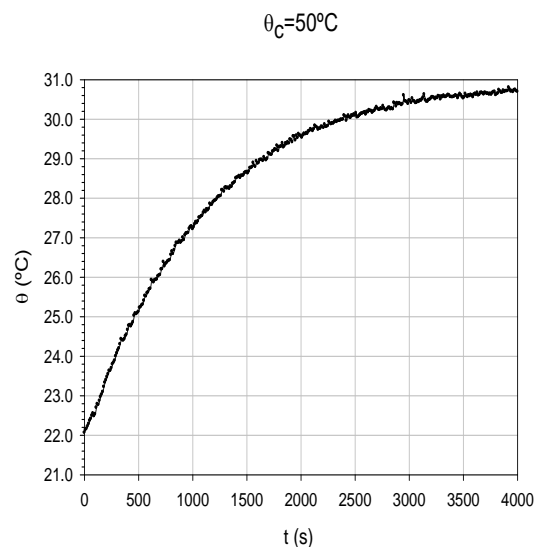

Figure 7. Thermogram for reference temperature θ_c =50ºC in the case of water (system: water + vessel + accessories).

Table 1: Results for the thermal scanning accomplishes in the case of a glass vessel with water placed on the heating cylinder. θ_r is the real temperature measures with infrared thermometer.

θ_c	θ_r	θ_a	θ_f	$\Delta\theta=(\theta_r-\theta_f)$	$\overline{C}=(\lambda_1+\lambda_2)$	$\overline{\theta}_f=(\lambda_1/\lambda_2)$	λ_1	λ_2	pot (w)	k_2 (w/mK)
30	29.5	18.9	23.0	6.5	0.0296	1.6185	0.0113	0.0183	0.3075	0.1028
35	34.1	21.3	25.2	8.9	0.0444	2.3058	0.0134	0.0310	0.5000	0.1222
40	39.4	21.9	27.2	12.2	0.0467	2.3153	0.0141	0.0326	0.7200	0.1283
45	44.4	22.0	28.8	15.6	0.0467	2.3080	0.0141	0.0326	0.9228	0.1286
50	49.5	21.9	30.7	18.8	0.0468	2.1542	0.0148	0.0319	1.1651	0.1350
55	54.3	23.1	32.8	21.5	0.0475	2.2179	0.0148	0.0327	1.3258	0.1344
60	59.1	23.1	34.1	24.9	0.0476	2.2570	0.0146	0.0330	1.5225	0.1330
65	63.7	23.5	35.4	28.3	0.0527	2.3776	0.0156	0.0371	1.8442	0.1420
70	68.4	23.5	36.6	31.7	0.0556	2.4113	0.0163	0.0393	2.1618	0.1483

From the thermograms for the system incorporating the problem material disk (PMD) between the heating element and the glass vessel containing water (Figure 5). The values of $\lambda_1{}^*$ and $\lambda_2{}^*$ were obtained for every temperature θ_c between 30 and 70°C (5°C steps), as well as the heating power $(\delta Q/\mathrm{d}t)^*$, whose values permit the determination of the disk thermal conductivity in accordance with (13). Figure 8 shows the corresponding thermogram at $\theta_c = 50$°C and Table 2 lists the results obtained when θ_c change over the range 30-70 °C using a PMD placed between the heating cylinder and the glass vessel with water.
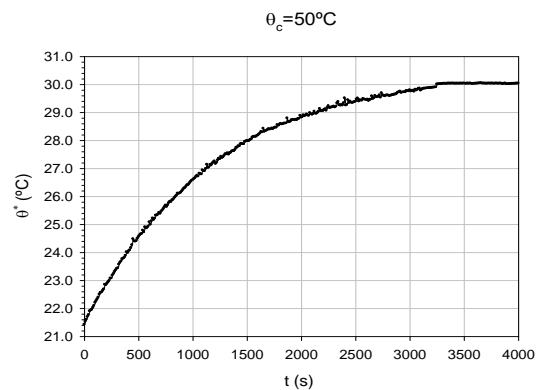
$\theta_c=50°C$

Figure 8. Water temperature vs. time when $\theta_c = 50$°C for the system disk +vessel+water+accesories.

Table 2: Problem plastic material disk: gain and loss parameters (λ_1 and λ_2), heating power (pot) and heat transmission coefficient (k_1) as a function of the measured temperature θ_f.

θ_c	$\theta_r{}^*$	θ_a	$\theta_f{}^*$	$\Delta\theta{}^* = (\theta_r{}^*-\theta_f{}^*)$	$\overline{C}{}^* = (\lambda_1{}^*+\lambda_2{}^*)$	$\overline{\theta}_f{}^* = (\lambda_1{}^*/\lambda_2{}^*)$	$\lambda_1{}^*$	$\lambda_2{}^*$	pot $*(w)$	k_1 (w/mK)
30	29.5	21.5	22.8	6.6	0.0399	5.1926	0.0064	0.0335	0.1794	0.1369
35	34.1	21.5	24.5	9.6	0.0384	3.1583	0.0092	0.0292	0.3705	0.2702
40	39.4	21.6	26.2	13.2	0.0412	2.8467	0.0107	0.0305	0.5898	0.4057
45	44.4	22.4	27.8	16.6	0.0438	3.1223	0.0106	0.0332	0.7376	0.3892
50	49.5	21.4	30.0	19.5	0.0465	2.2575	0.0143	0.0322	1.1618	3.5232
55	54.3	21.8	31.7	22.6	0.0467	2.2813	0.0142	0.0324	1.3441	3.5283
60	59.1	22.0	33.0	26.1	0.0467	2.3859	0.0138	0.0329	1.5068	2.2718
65	63.7	21.9	34.2	29.5	0.0467	2.4015	0.0137	0.0330	1.6955	1.0466
70	68.4	22.3	35.5	32.9	0.0469	2.5060	0.0134	0.0335	1.8419	0.6835

Figures 9 and 10 depict the meshes corresponding to the thermal behavior of each of the systems (water and PMD). Heating raises the temperature from environmental temperature (θ_a) to the final temperature (θ_f) corresponding to the steady state.
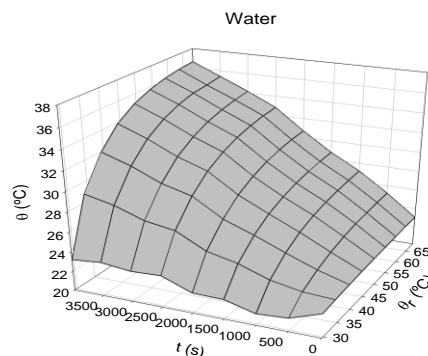
Water

Figure 9. Mesh for thermal behavior for the system (glass + water + accessories)
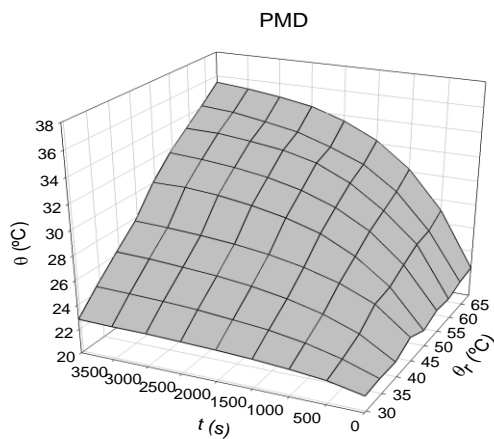
PMD

Figure 10. Mesh for thermal behavior for the system (PMD + glass + water + accessories)

Figures 11 and 12 show the values of the heating power and heat transmission coefficient corresponding to the glass of the vessel used (system without PMD), while Figures 13 and 14 correspond to the same quantities when PMD is used. In the last case the values obtained for the heat transmission coefficient show a clear peak suggesting out some type of internal structure transition for the PMD between 28 and 34ºC.
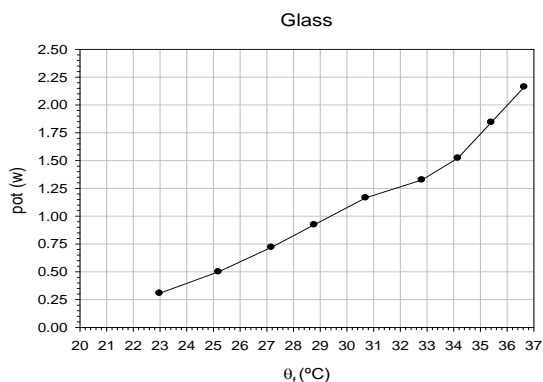
Glass

Figure 11. Heating power for the system glass +water+accessories *vs.* temperature.
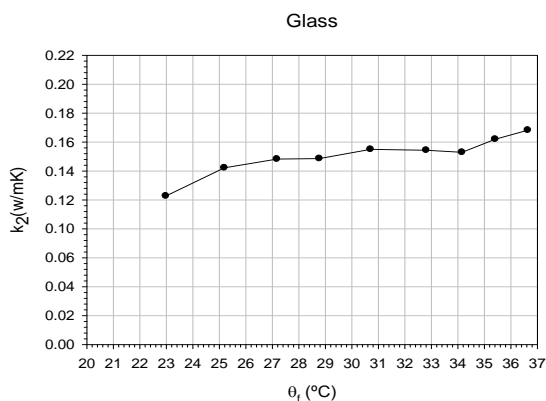
Glass

Fígure 12. Heat transmission coefficients for water *vs.* temperature.
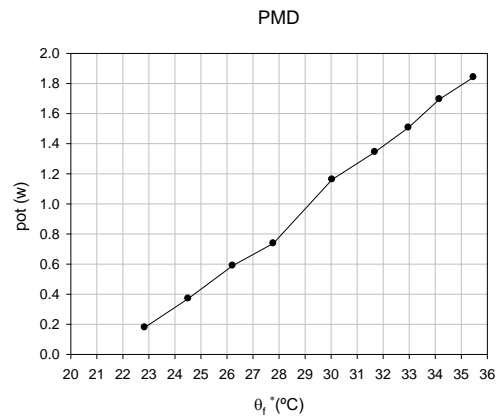
PMD

Figure 13. Heating power for the complete system PMD+glass+water+accessories *vs.* temperature.
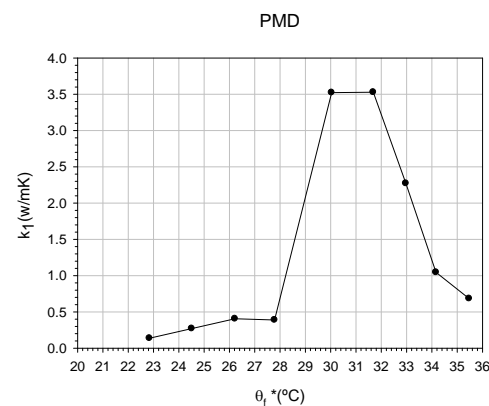
PMD

Figure 14. Heat transmission coefficients for PMD *vs.* temperature. Note the peak zone at 30-32ºC.

REFERENCES

[1]. A. Hein, N.S. Müller, P.M. Day, V. Kilikoglou, Thermal conductivity of archaeological ceramics: The effect of inclusions, porosity and firing temperature, Thermochimica Acta **480**, 35 (2008).

[2]. A. Hein, I. Karatasios, N.S. Müller, V. Kilikoglou, Heat transfer properties of pyrotechnical ceramics used in ancient metallurgy, Thermochimica Acta **573**, 87 (2013).

[3]. D. Li, M.A. Wells, Effect of subsurface thermocouple installation on the discrepancy of the measured thermal history and predicted surface heat flux during a quench operation, Metallurgical and Materials Transactions B: Process Metallurgy and Materials Processing Science **36** (3), 343 (2005).

[4]. A.V. Murthy, G.T. Fraser, D.P. DeWitt, A summary of heat-flux sensor calibration data, Journal of Research of the National Institute of Standards and Technology **110** (2), 97 (2005).

[5]. D.A. Gonzalez *et al.*, Defect assessment on

radiant heaters using infrared thermography, NDT and E. International **38** (6), 428 (2005).

[6]. A.D. Ochoa, J.W. Baughn, A.R. Byerley, A new technique for dynamic heat transfer measurements and flow visualization using liquid crystal thermography, International Journal of Heat and Fluid Flow **26** (2), 264 (2005).

[7]. J. Fernandez-Seara *et al*., Experimental apparatus for measuring heat transfer coefficients by the Wilson plot method, European Journal of Physics **26** (3), 1 (2005).

[8]. Y. Heichal, S. Chandra, E. Bordatchev, A fast-response thin film thermocouple to measure rapid surface temperature changes, Experimental Thermal and Fluid Science **30** (2), 153 (2005).

[9]. T.A. Shedd, B.W. Anderson, An automated non-contact wall temperature measurement using thermoreflectance, Measurement Science and Technology **16** (12), 2483 (2005).

[10]. Y. Liu, X. Zhang, Influence of participating media on the radiation thermometry for surface temperature measurement, Journal of Thermal Science **14** (4), 368 (2005).

[11]. S. Welzel, H.W. Gronert, E.F. Wassermann, D.M. Herlach, Influence of the preparation conditions on the thermal conductivity in metallic glasses, Materials Science and Engineering: A **145** (1), 119 (1991).

[12]. B. Chowdhury, S.C. Mojumdar, Aspects of thermal conductivity relative to heat flow, Journal of Thermal Analysis and Calorimetry **81** (1), 179 (2005).

[13]. W.N. Dos Santos, Thermal properties of melt polymers by the hot wire technique, Polymer Testing **24** (7), 932 (2005).

[14]. F. Frusteri *et al*., Thermal conductivity measurement of a PCM based storage system containing carbon fibers, Applied Thermal Engineering **25** (11-12), 1623 (2005).

[15]. B. Kshirsagar *et al*., Thermal contact conductance across gold-coated OFHC copper contacts in different media, Journal of Heat Transfer **127** (6), 657 (2005).

[16]. B. Remy, A. Degiovanni, D. Maillet, Measurement of the in-plane thermal diffusivity of materials by infrared thermography, International Journal of Thermophysics **26** (2), 493 (2005).

[17]. M.C. Garcia-Payo, M.A. Izquierdo-Gil, Thermal resistance technique for measuring the thermal conductivity of thin microporous membranes, Journal of Physics D-Applied Physics **37** (21), 3008 (2004).

[18]. N. Sombatsompop, A.K. Wood, Measurement of thermal conductivity of polymers using an improved Lee's Disc apparatus, Polymer Testing **16** (3), 203 (1997).

[19]. D.M Price, M. Jarratt, Thermal conductivity of PTFE and PTFE composites, Thermochimica Acta **392–393**, 231 (2002).

[20]. A., Nidaa, Effect of Heat Treatment On Tensile Strength, Hardness and Thermal conductivity of Blended Polymer Composite, Proceedings of 7th International Conference on Processing and Manufacturing of Advanced Materials, Quebec City, CANADA, 2012, edited by T. Chandra, M. Ionescu, D. Mantovani, (Ed.), Vol. **706** (Quebec City, CANADA, 2012).

[21]. S. Mahesh, S.C. Joshi, Thermal conductivity variations with composition of gelatin-silica aerogel-sodium dodecyl sulfate with functionalized multi-walled carbon nanotube doping in their composites, International Journal of Heat and Mass Transfer **87**, 606 (2015).

[22]. M. Rides, J. Morikawa, L. Halldahl, B. Hay, H. Lobo, A. Dawson, C. Allen, Intercomparison of thermal conductivity and thermal diffusivity methods for plastics, Polymer Testing **28**, 480 (2009).

[23]. N. Sombatsompop, A.K. Wood, Measurement of Thermal Conductivity of Polymers using an Improved Lee's Disc Apparatus, Polymer Testing **16**, 203 (1997).

[24]. O.S. Samuel, B.O. Ramon, Y.O. Johnson, Thermal Conductivity of Three Different Wood Products of Combretaceae Family; Terminalia superb, Terminalia ivorensis and Quisqualis indica, Journal of Natural Sciences Research **2** (9), 18 (2012).

[25]. M. Alam, S. Rahman, P.K. Halder, A. Raquib, M. Hasan, Lee's and Charlton's Method for Investigation of Thermal Conductivity of Insulating Materials, Journal of Mechanical and Civil Engineering **3** (1), 53 (2012).

[26]. P. Philip, L. Fagbenle, Design of lee's disc electrical method for determining thermal conductivity of a poor conductor in the form of a flat disc, International Journal of Innovation and Scientific Research **9** (2), 335 (2014).

[27]. J.A. Ibáñez, M.R. Ortega, *Lecciones de Física. Termología 1*, (DM Ediciones, Murcia, 2003).